Structure of the 1,N^2-Ethenodeoxyguanosine Adduct Opposite Cytosine in Duplex DNA: Hoogsteen Base Pairing at pH 5.2†

Ganesh Shanmugam,‡ Ivan D. Kozekov,‡ F. Peter Guengerich,§ Carmelo J. Rizzo,‡,§ and Michael P. Stone*,‡,§

Departments of Chemistry and Biochemistry, Vanderbilt Institute of Chemical Biology, Center in Molecular Toxicology and the Vanderbilt-Ingram Cancer Center, Vanderbilt University, Nashville, Tennessee 37235

Received April 23, 2008

The exocyclic 1,N^2-ethenodeoxyguanosine (1,N^2-ϵdG) adduct, arising from the reaction of vinyl halides and other vinyl monomers, including chloroacetaldehyde, and lipid peroxidation products with dG, was examined at pH 5.2 in the oligodeoxynucleotide duplex 5′-d(CGCATXGAATCC)-3′•5′-d(GGATTC-CATGCG)-3′ (X = 1,N^2-ϵdG). Previously, X(*anti*)•C(*anti*) pairing was established in this duplex, containing the 5′-TXG-3′ sequence context, at pH 8.6 [Shanmugam, G., Goodenough, A. K., Kozekov, I. D., Harris, T. M., Guengerich, F. P., Rizzo, C. J., and Stone, M. P. (2007) *Chem. Res. Toxicol. 20*, 1601−1611]. At pH 5.2, the 1,N^2-ϵdG adduct decreased the thermal stability of the duplex by ∼13 °C. The 1,N^2-ϵdG adduct rotated about the glycosyl bond from the *anti* to the *syn* conformation. This resulted in the observation of a strong nuclear Overhauser effect (NOE) between the imidazole proton of 1,N^2-ϵdG and the anomeric proton of the attached deoxyribose, accompanied by an NOE to the minor groove A^{20} H2 proton from the complementary strand. The *syn* conformation of the glycosyl bond at 1,N^2-ϵdG placed the exocyclic etheno moiety into the major groove. This resulted in the observation of NOEs between the etheno protons and the major groove protons of the 5′-neighboring thymine. The 1,N^2-ϵdG adduct formed a Hoogsteen pair with the complementary cytosine, characterized by downfield shifts of the amino protons of the cytosine complementary to the exocyclic adduct. The pattern of chemical shift perturbations indicated that the lesion introduced a localized structural perturbation involving the modified base pair and its 3′- and 5′-neighbor base pairs. A second conformational equilibrium was observed, in which both the modified base pair and its 3′-neighboring G•C base pair formed tandem Hoogsteen pairs. The results support the conclusion that at neutral pH, in the 5′-TXG-3′ sequence, the 1,N^2-ϵdG adduct exists as a blend of conformations in duplex DNA. These involve the interconversion of the glycosyl torsion angle between the *anti* and the *syn* conformations, occurring at an intermediate rate on the NMR time scale.

Introduction

Ethenobases are five-membered exocyclic addition products to DNA nucleobases. The etheno ring system is found in DNA adducts (*1*) arising from the reactions of electrophiles derived from vinyl halides and other vinyl monomers, including chloroacetaldehyde, with dC, dA, and dG nucleotides in DNA (*2–9*). They also arise as a consequence of endogenous exposure to lipid peroxidation products (*10*), particularly 4,5-epoxy-2(*E*)-decanal and 4-oxo-2(*E*)-nonenal (*11–14*), and 9,12-dioxo-10(*E*)-dodecanoic acid (*15, 16*). The 1,N^2-ethenodeoxyguanosine (1,N^2-ϵdG)[1] adduct (Scheme 1) (*17*) is one of two possible ϵdG lesions, the other being the N^2,3-ethenodeoxyguanosine (N^2,3-ϵdG) adduct. The Guengerich laboratory elucidated the mechanism for the formation of 1,N^2-ϵdG (*18, 19*). It has been detected in DNA treated with vinyl chloride metabolites (*20*)

Scheme 1. (A) 1,N^2-ϵdG-Modified Oligodeoxynucleotide Numbering Scheme and (B) Structure and Numbering Scheme for 1,N^2-ϵdG Adduct[a]

A

5′-C^1 G^2 C^3 A^4 T^5 X^6 G^7 A^8 A^9 $T^{10}$$C^{11}$$C^{12}$-3′

3′-$G^{24}$$C^{23}$$G^{22}$$T^{21}$$A^{20}$$C^{19}$$C^{18}$$T^{17}$$T^{16}$$A^{15}$$G^{14}$$G^{13}$-5′

B

X =

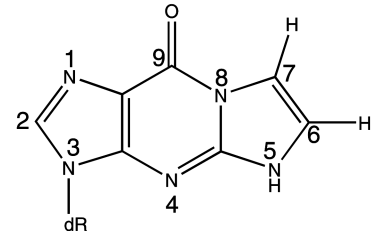

[a] 1,N^2-ϵdG. The imidazole proton of the 1,N^2-ϵdG nucleotide is designated as H2, corresponding to the H8 proton in guanine.

† This paper is dedicated to the memory of Professor Bea Singer (1922−2005).

* To whom correspondence should be addressed. Tel: 615-322-2589. Fax: 615-322-7591. E-mail: michael.p.stone@vanderbilt.edu.

‡ Department of Chemistry.

§ Department of Biochemistry.

[1] Abbreviations: 1,N^2-ϵdG, 1,N^2-ethenodeoxyguanosine; N^2,3-ϵdG, N^2,3-ethenodeoxyguanosine; 1,N^2-PdG, 1,N^2-propanodeoxyguanosine; 1,N^6-ϵdA, 1,N^6-ethenodeoxyadenosine; 3,N^4-ϵdC, 3,N^4-ethenodeoxycytosine; NOE, nuclear Overhauser enhancement; NOESY, two-dimensional NOE spectroscopy; COSY, correlation spectroscopy; ppm, parts per million; TPPI, time proportional phase increment; 1D, one-dimensional; 2D, two-dimensional; CGE, capillary gel electrophoresis. A right superscript refers to the numerical position in the sequence starting from the 5′ terminus of chain A and proceeding to the 3′ terminus of chain A and then from the 5′ terminus of chain B to the 3′ terminus of chain B. C2, C5, C6, C8, C1′, C2′, etc. represent specific carbon nuclei. H2, H5, H6, H8, H1′, H2′, H2″, etc. represent protons attached to these carbons.

10.1021/tx8001466 CCC: $40.75
Published on Web 08/12/2008

and β-carotene oxidation products (*21*) and has been isolated using immunohistochemistry (*22*) and high-sensitivity mass spectrometric techniques from liver DNA in rodents (*23–25*).

The 1,N^2-ϵdG adduct is mutagenic, both in *Escherichia coli* (*26*) and in mammalian (*27*) cells. When bypassed by *E. coli* polymerases I *exo-* and II *exo-*, T7 polymerase *exo-*, HIV-1 reverse transcriptase, and rat polymerase β, it produces misincorporation errors (*28*). The bypass of the 1,N^2-ϵdG adduct by the Y-family *Sulfolobus solfataricus P2* DNA polymerase IV (Dpo4) was dependent upon the DNA sequence. When the template was 3′-(1,N^2-ϵdG)TACT-5′, dATP was preferentially incorporated, whereas with the template 3′-(1,N^2-ϵdG)CACT-5′, both dGTP and dATP were incorporated (*29*). The replicative human polymerase pol δ was blocked by the 1,N^2-ϵdG adduct (*30*). Human polymerase η conducts error-prone replication past 1,N^2-ϵdG, preferentially incorporating dGTP opposite the adduct, irrespective of the identity of the base 5′ of 1,N^2-ϵdG in the template (*30*). The human polymerases ι and κ showed similar rates of incorporation of dTTP and dCTP (*30*).

The insertion of the 1,N^2-ϵdG lesion into a template containing the 5′-TXG-3′ sequence and the formation of either binary or ternary complexes with the *S. solfataricus* DNA polymerase Dpo4 were reported by Zang et al. (*29*). To compare the structure of 1,N^2-ϵdG in duplex DNA with that in the binary and ternary polymerase complexes, 1,N^2-ϵdG was inserted into the duplex 5′-d(CGCATXGAATCC)-3′•5′-d(GGATTCCATGCG)-3′ (X = 1,N^2-ϵdG) (Scheme 1) containing the 5′-TXG-3′ sequence context. A refined structure of the 1,N^2-ϵdG adduct has been reported at neutral pH in the 5′-CXC-3′ sequence (*31*), but in the 5′-TXG-3′ sequence, at neutral pH, spectral line broadening arising from conformational exchange precluded structural refinement (*32*). However, at pH 8.6 in the 5′-TXG-3′ sequence context, it was possible to obtain well-resolved ^{1}H NMR spectra (*32*). The 1,N^2-ϵdG-induced structural perturbation was localized at the X^6•C^{19} base pair and its 5′-neighbor T^5•A^{20}. Both the 1,N^2-ϵdG and the complementary dC adopted the *anti* conformation about the glycosyl bonds. The 1,N^2-ϵdG adduct was inserted into the duplex; however, the etheno moiety oriented toward the minor groove. The complementary cytosine was displaced toward the major groove. The 5′-neighboring T^5•A^{20} base pair exhibited a disruption in Watson−Crick base pairing (*32*).

The present work examines the 1,N^2-ϵdG-adducted oligodeoxynucleotide duplex, containing the 5′-TXG-3′ sequence context, at pH 5.2. At the lower pH, the 1,N^2-ϵdG adduct introduces a localized perturbation at the modified base pair X^6•C^{19} and its 3′-neighboring base pair G^7•C^{18}. The 1,N^2-ϵdG adduct rotates about the glycosyl bond into the *syn* conformation, placing the exocyclic adduct into the major groove. The 1,N^2-ϵdG adduct forms a Hoogsteen pair with the complementary nucleotide C^{19}, as was suggested by Zaliznyak et al. (*31*). A second conformational equilibrium is observed, in which the 3′-neighboring G•C base pair also transitions to a Hoogsteen pair.

Materials and Methods

The oligodeoxynucleotides 5′-d(CGCATGGAATCC)-3′ and 5′-d(GGATTCCATGCG)-3′ were synthesized and purified by anion-exchange chromatography by the Midland Certified Reagent Co. (Midland, TX). The 1,N^2-ϵdG phosphoramidite (*33*) was incorporated into 5′-d(CGCATXGAATCC)-3′ (X = 1,N^2-ϵdG) oligodeoxynucleotide using an Expedite 8909 DNA synthesizer (PerSeptive Biosystems) on a 1 μmol scale using the manufacturer's standard protocols. Following cleavage of the modified oligodeoxynucleotide from the solid support, the exocyclic amino groups were deprotected using 0.1 M aqueous NaOH at room temperature overnight. The deprotection reaction was neutralized, and the oligodeoxynucleotide was purified by HPLC, using a Beckman HPLC system with UV detection at 260 nm with Waters YMC ODS-AQ columns (250 mm × 10 mm i.d., 5 mL/min). The gradient was initially 1% CH_3CN; 5 min linear gradient to 8% CH_3CN; 15 min linear gradient to 11% CH_3CN; 2 min linear gradient to 80% CH_3CN; 1 min isocratic at 80% CH_3CN; and 2 min linear gradient to initial conditions. The oligodeoxynucleotide was desalted over Sephadex G-25 using a BioRad FPLC system and analyzed by capillary gel electrophoresis (CGE) (99.5%) using a Beckman P/ACE MDQ instrument system with a 31.2 cm × 100 μm eCAP capillary; samples were applied at 10 kV and run at 9 kV and detected at 260 nm. The capillary was packed with the manufacturer's 100-R gel (for ss-DNA) using a tris-borate buffer system containing 7 M urea. MALDI-TOF mass spectra (negative ion) of modified oligodeoxynucleotides were obtained on a Voyager Elite DE instrument (Perseptive Biosystems) at the Vanderbilt Mass Spectrometry Facility using a 3-hydroxypicolinic acid matrix containing ammonium hydrogen citrate (7 mg/mL) to suppress multiple Na^+ and K^+ adducts. 5′-d(CGCATXGAATCC)-3′, MALDI-TOFMS: calcd for $[M - H]^-$, *m/z* 3652.6; found, *m/z* 3653.0.

Enzymatic Digestion. The oligodeoxynucleotide (0.5 A_{260} units) was dissolved in 30 μL of buffer (pH 7.0, 10 mM Tris-HCl and 10 mM $MgCl_2$) and incubated with DNase I (8 units, Promega), snake venom phosphodiesterase I (0.02 units, Sigma), and *E. coli* alkaline phosphatase (1.7 units, Sigma) at 37 °C for 24 h. The mixture was analyzed by HPLC with UV detection at 260 nm and a Waters YMC ODS-AQ column (250 mm × 4.6 mm i.d., 1.5 mL/min). The gradient was initially 1% CH_3CN; 15 min linear gradient to 10% CH_3CN; 5 min linear gradient to 20% CH_3CN; 5 min isocratic at 20% CH_3CN; 3 min linear gradient to 80% CH_3CN; 2 min isocratic at 80% B; and 3 min linear gradient to initial conditions. The adducted nucleoside was identified by comparison with an authentic sample based on retention times, coinjection, and its UV spectrum.

Thermal Denaturation Studies. Experiments were conducted on a Cary 4E spectrophotometer (Varian Associates, Palo Alto, CA). The samples contained 0.33 A_{260} unit of duplex oligodeoxynucleotide dissolved in 1 mL of buffer containing 10 mM Na_2HPO_4/NaH_2PO_4, 1.0 M NaCl, and 5 μM Na_2EDTA (pH 5.2). The absorbance at 260 nm was monitored at 1 min intervals with a 2.5 °C/min temperature gradient. The temperature was cycled between 20 and 85 °C. The first derivative of the melting curve was used to establish the T_m values.

NMR. Samples were dissolved to a duplex concentration of 1 mM in 500 μL of buffer containing 10 mM NaH_2PO_4, 100 mM NaCl, and 5 μM Na_2EDTA (pH 5.2; uncorrected for deuterium isotope effects). Samples for the observation of nonexchangeable protons were exchanged with D_2O and suspended in 500 μL of 99.99% D_2O. Samples for the observation of exchangeable protons were dissolved to a concentration of 1 mM in 500 μL of buffer containing 10 mM NaH_2PO_4, 100 mM NaCl, and 5 μM Na_2EDTA (pH 5.2) 9:1 H_2O:D_2O (v/v). The pH was adjusted by titration with either DCl or NaOD. Chemical shifts of the proton resonances were referenced to water. For experiments in which the 1,N^2-ϵdG H7 etheno proton was exchanged with deuterium, the 1,N^2-ϵdG-modified oligodeoxynucleotide duplex was suspended in 500 μL of D_2O, containing 10 mM NaH_2PO_4, 100 mM NaCl, and 5 μM Na_2EDTA (pH 8.6). To achieve complete exchange of H7 proton, the sample was kept at 50 °C for ∼96 h. The pH was adjusted to pH 5.2 (uncorrected for deuterium isotope effects) using a dilute solution of DCl.

NMR spectra were recorded on Bruker Avance spectrometers operating at 600 and 800 MHz and at 7 °C. For each t_1 increment of ^{1}H two-dimensional (2D) NOE spectroscopy (NOESY) experiments in D_2O, 32 scans were averaged with presaturation of the HDO resonance. Spectra were recorded consecutively using time proportional phase increment (TPPI) phase cycling with mixing times of 70, 150, 200, and 250 ms. These were recorded with 2048 complex points in the acquisition dimension and 1024 real data

points in the indirect dimension covering 9615.385 Hz. The relaxation delay was 1.5 s. The data in the d_2 dimension were zero-filled to give a matrix of 2K × 2K real points. NOESY spectra for observation of exchangeable protons were recorded in 9:1 H_2O:D_2O (v/v), using the Watergate pulse sequence (*34*) for water suppression. The spectra, consisting of 128 transients, were obtained with a cryogenic probe using States-TPPI phase cycling with a mixing time of 250 ms. A squared sine-bell with 72° shift apodization was applied in d_1 dimension while cosine-squared bell apodization was applied in the d_2 dimension. A total of 1536 real data points in the d_1 dimension and 512 points in d_2 dimension were acquired. Chemical shifts of proton resonances were referenced to water. NMR data were processed on Silicon Graphics Octane workstations and assigned using FELIX2000 (Accelrys, Inc., San Diego, CA).

Molecular Modeling. Potential energy minimization calculations were conducted with the program X-PLOR (*35*). Classical B-DNA (*36*) was used as the reference structure to create starting structures for the calculations. The program INSIGHT II (Accelrys Technologies, Inc., San Diego, CA) was used to build the initial structures and for visualization of minimized structures. The 1,N^2-ϵdG adduct was constructed by bonding the etheno group to N1 and N^2 at G^6 using INSIGHT II. The restrained electrostatic potential (RESP) charges for the 1,N^2-ϵdG adduct and the protonated cytosine were calculated using the program GAUSSIAN98 (*37*) on the free bases (excluding the sugar−phosphate portion) using a total charge of +1 for protonated cytosine and a neutral charge on 1,N^2-ϵdG adduct. The input data for the GAUSSIAN98 calculations were obtained from the program ANTECHAMBER (*38*).

Results

Characterization of the Modified Duplex. At neutral pH, 1,N^2-ϵdG induced a 14 °C decrease in T_m. It was not possible to examine the 1,N^2-ϵdG adduct positioned opposite dC at neutral pH by NMR due to the existence of broad peaks in the modified region of the duplex. This was attributed to the presence of multiple conformations of the 1,N^2-ϵdG adduct at neutral pH (*32*). However, decreasing the pH of the sample to pH 5.2 yielded a reasonably well-resolved NMR spectrum. Therefore, the work described here focuses on the 1,N^2-ϵdG adduct at pH 5.2. The T_m of the modified duplex was 40 °C in 10 mM NaH_2PO_4, 100 mM NaCl, and 5 μM Na_2EDTA (pH 5.2). The corresponding T_m for the unmodified duplex under the same conditions was 53 °C. Thus, 1,N^2-ϵdG induced a ∼13 °C decrease in T_m.

Resonance Assignments. 1. Nonexchangeable Protons. For the modified strand, the anticipated pattern of sequential base aromatic→deoxyribose anomeric nuclear Overhauser enhancement (NOE) was identified from C^1→T^5 (Figure 1A). The A^4 H1′→T^5 H6 and T^5 H6→T^5 H1′ NOEs were weak. The T^5 H1′→X^6 H2 NOE (the imidazole proton of 1,N^2-ϵdG; note the modified numbering scheme for this nucleotide) was missing, interrupting the NOE connectivity. The intensity of the X^6 H2→X^6 H1′ cross-peak was exceptionally large. The X^6 H1′→G^7 H8 NOE was weak. The G^7 H8→G^7 H1′ and the G^7 H1′→A^8 H8 NOEs were not detected. Figure 1B shows the phase-sensitive NOESY spectrum with a 70 ms mixing time. The strong cross-peak assigned to the X^6 H2→X^6 H1′ NOE remained present at the shorter mixing time. Proceeding in the 3′-direction from the A^8 H8→A^8 H1′ NOE, the NOESY connectivities continued uninterrupted to the 3′ terminus of the modified strand. In the complimentary strand, the NOE connectivities were continuous (Figure 1C). However, the resonances of C^{19}, the nucleotide complimentary to X^6, were broad. The C^{18} H6→C^{18} H1′ and C^{18} H1′→C^{19} H6 cross-peaks overlapped with the C^{12} H6→C^{11} H1′ and C^{11} H6→C^{11} H1′ NOE cross-peaks, respectively. Similarly, the C^{19} H6→C^{19} H1′ cross-peak overlapped with the C^{19} H5→C^{19} H6 cross-peak. The C^{19} H1′→A^{20} H8 NOE was weak. The pattern of NOEs between the base aromatic protons and the deoxyribose H2′ and H2″ protons was similar to that observed for the NOEs between the aromatic protons and the deoxyribose H1′ protons, in both the modified and the complementary strands. Sequential NOEs were disturbed from T^5 to G^7 in the modified strand and from

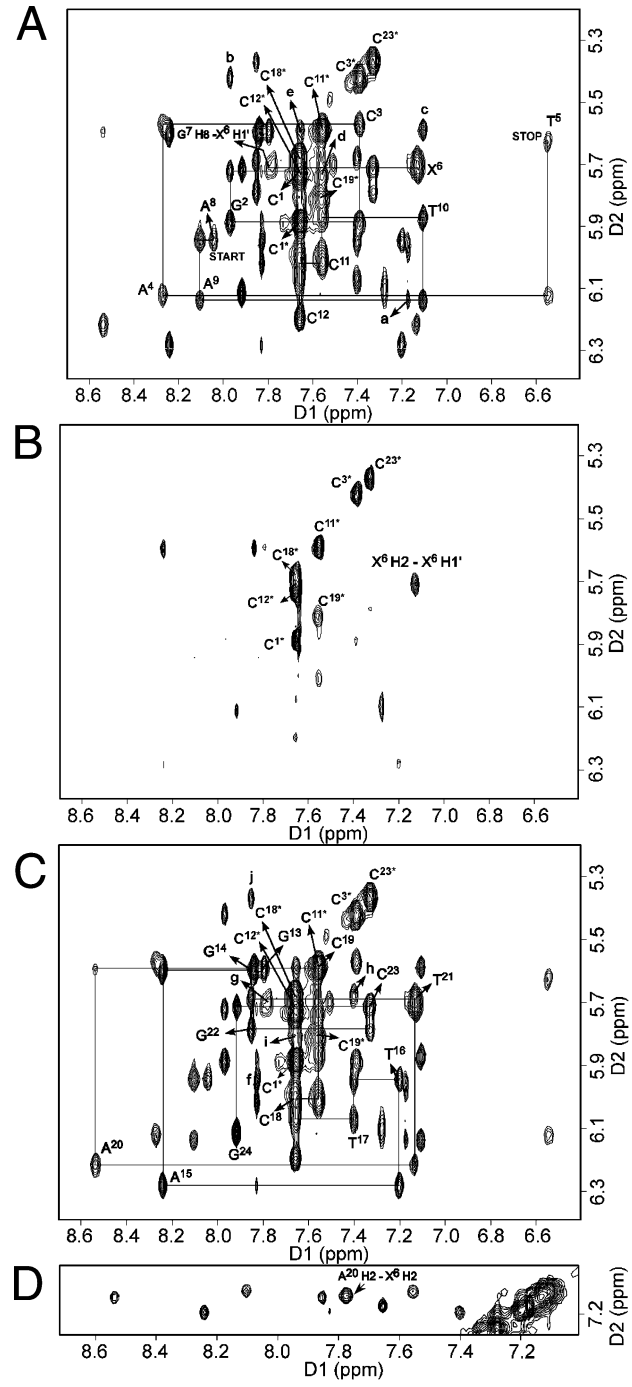

Figure 1. ^{1}H NOESY spectrum collected at 250 ms mixing time at 7 °C (pH 5.2). (A) Sequential NOE connectivity from anomeric H1′ to 3′-neighbor aromatic protons of the modified strand. Peaks: a, A^8 H2→A^9 H1′; b, G^2 H8→C^3 H5; c, T^{10} H6→C^{11} H5; d, C^{11} H6→C^{12} H5; and e, C^{12} H6→C^{11} H5. (B) ^{1}H NOESY spectrum collected at a NOE mixing time of 70 ms showing the X^6 H2→X^6 H1′ NOE. (C) Sequential NOE connectivity from anomeric H1′ to 3′-neighbor aromatic protons for the complimentary strand. Labeled peaks: f, A^{15} H2→T^{16} H1′; g, A^{20} H2→T^{21} H1′; h, T^{17} H6→C^{18} H5; i, C^{18} H6→C^{19} H5; and j, G^{22} H8→C^{23} H5. (D) The 5′-purine H8→3′-pyrimidine H6 NOEs showing an additional NOE that was assigned as A^{20} H2→X^6 H2. Asterisks indicate the cytosine H5−H6 cross-peaks.

C^{18} to A^{20} in the complimentary stand (Figure S1 of the Supporting Information).

An expansion of the ^{1}H NOESY spectrum showing the 5′→3′ NOEs between purine H8/pyrimidine H6 protons is shown in Figure 1D. An additional cross-peak was observed at 7.12 parts per million (ppm), assigned as an NOE between the minor groove A^{20} H2 proton and the imidazole proton of 1,N^2-ϵdG, A^{20} H2→X^6 H2. The anticipated sequential 5′→3′ NOEs between purine H8/pyrimidine H5 protons in the G^2→C^3 (peak b, Figure 1A), T^{10}→C^{11} (peak c, Figure 1A), C^{11}→C^{12} (peak d, Figure 1A), T^{17}→C^{18} (peak h, Figure 1C), C^{18}→C^{19} (peak i, Figure 1C), and G^{22}→C^{23} (peak j, Figure 1C) steps were observed. Anticipated NOEs between purine H8 and thymine CH_3 protons were observed for the A^4→T^5, A^9→T^{10}, A^{15}→T^{16}, T^{16}→T^{17}, and A^{20}→T^{21} steps. The sequential A^4 H2→T^5 H1′ (not observed at the contour level plotted in Figure 1A), A^8 H2→A^9 H1′ (peak a, Figure 1A), A^9 H2→T^{10} H1′ (overlapped), A^{15} H2→T^{16} H1′ (peak f, Figure 1C), and A^{20} H2→T^{21} H1′ (peak g, Figure 1C) NOEs were observed. While the H3′ and H4′ resonances could be assigned, the diastereotopic assignments of the H5′ and H5″ resonances remained equivocal. The assignments of the nonexchangeable protons for the unmodified and modified duplexes at pH 5.2 are summarized in Tables S1 and S2 in the Supporting Information, respectively. For the unmodified duplex, the sequential NOE connectivity between aromatic protons and 3′-neighbor deoxyribose H1′ protons at pH 5.2 is presented in Figure S2 in the Supporting Information.

2. Exchangeable Protons. The assignments for the DNA imino protons are shown in Figure 2A. Five partially overlapped resonances, located between 13.2 and 13.8 ppm, arose from thymine N3H protons, as evidenced by NOEs to the corresponding adenine H2 protons (Figure 2B). Similarly, three resonances between 12.5 and 13.2 ppm arose from guanosine N1H protons. The resonance at 13.0 ppm was assigned to G^2 N1H based on the NOEs to the complementary C^{23} amino protons (Figure 2B). The anticipated pattern of sequential NOE connectivities was observed from base pairs G^2•C^{23}→T^5•A^{20} (Figure 2C). It was interrupted between base pairs T^5•A^{20} and X^6•C^{19} and between base pairs X^6•C^{19} and G^7•C^{18}. The weak resonance located at 12.3 ppm was assigned as G^7 N1H, by observation of the sequential NOE to base pair A^8•T^{17}. The anticipated NOEs between the G^7 N1H and the amino protons of the complementary nucleotide C^{18} were not detected. Sequential NOE connectivities were observed from G^7•C^{18}→C^{11}•G^{14} base pairs (Figure 2C).

Additional resonances were observed (Figure 2A). Two resonances were observed at 9.0 and 10.2 ppm and assigned to the amino protons of protonated C^{19}, which is complementary to X^6. These were assigned by observation of NOEs to C^{19} H5 (Figure 3). The downfield resonance was assigned to hydrogen-bonded amino proton, and the upfield resonance was nonhydrogen-bonded amino proton of C^{19}. These assignments were confirmed by the observation of weak NOEs between each of the C^{19} amino protons and the Watson−Crick hydrogen-bonded imino proton of the 5′-neighbor T^5•A^{20} base pair (Figure S3 in the Supporting Information). Two additional weak signals were also observed at 9.6 and 10.6 ppm (Figure 2A). These were assigned to a second conformational equilibrium of the adducted duplex, in which the 3′-neighbor base pair also was shifting to the Hoogsteen conformation (vide infra). Two weak peaks were observed at 14.8 and 15.4 ppm (Figure 2A). They were assigned as arising from protonation of C^{18} and C^{19} at the N3 position. The resonance assigned as C^{19} $N3H^+$ was of greater intensity than that assigned as C^{18} $N3H^+$. The resonance assignments

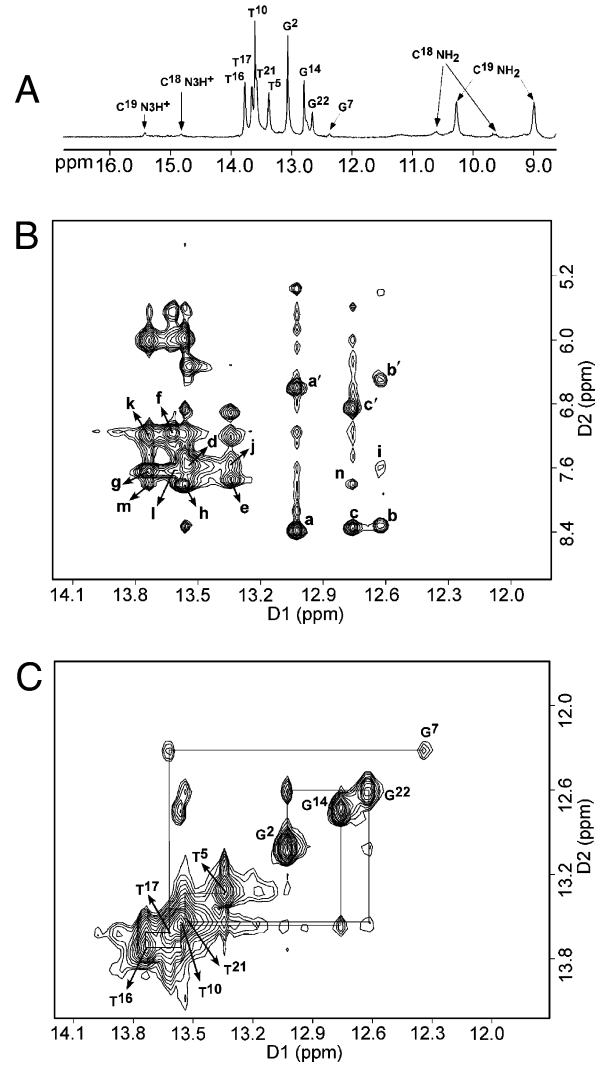

Figure 2. (A) Downfield region of the ^{1}H NMR spectrum recorded in buffer solution containing 9:1 H_2O:D_2O at 7 °C (pH 5.2). (B) ^{1}H NOESY spectrum showing the NOE connectivity between the imino protons and the amino and base protons. Labeled peaks: a,a′, G^2 N1H→C^{23} N^4H, h/n; b,b′, G^{22} N1H→C^3 N^4H, h/n; c,c′, G^{14} N1H→C^{11} N^4H, h/n; d, T^{21} N3H→A^4 H2; e, T^5 N3H→A^{20} H2; f, T^{17} N3H→A^8 H2; g, T^{16} N3H→A^9 H2; h, T^{10} N3H→A^{15} H2; i, G^{22} N1H→A^4 H2; j, T^5 N3H→A^4 H2; k, T^{16} N3H→A^8 H2; l, T^{17} N3H→A^9 H2; m, T^{16} N3H→A^{15} H2; and n, G^{14} N1H→A^{15} H2. The symbols h and n stand for hydrogen-bonded and nonhydrogen-bonded amino protons of cytosine. (C) ^{1}H NOESY spectrum showing resonances for the thymine and guanine imino protons and sequential NOE connectivity for the imino protons of base pairs G^2•C^{23}→G^{14}•C^{11}. The labels designate the imino proton of the indicated nucleotide. The spectra were recorded in 9:1 H_2O:D_2O at 7 °C (pH 5.2).

for the imino and amino protons of the 1,N^2-ϵdG-adducted and the corresponding unmodified duplexes are found in Tables S3 and S4, respectively, in the Supporting Information.

3. Assignment of the 1,N^2-ϵdG Etheno Protons. The etheno protons exhibit a small *J* coupling constant, 2.6 Hz for the nucleoside (*33, 39, 40*), which precludes their observation in correlation spectroscopy (COSY) type experiments at the oligodeoxynucleotide level. Surprisingly, NOESY spectra also did not show a strong NOE peak for the etheno protons, despite their strong dipolar coupling interaction. This was attributed to spectral overlap of the etheno H6 and H7 protons, which was confirmed by selective deuteration of the H7 proton (*18*). Figure 4 shows an overlay of two NMR spectra, before and after deuteration of the H7 proton. For the deuterated sample at pH 5.2, the integrated intensity of the resonance assigned to the

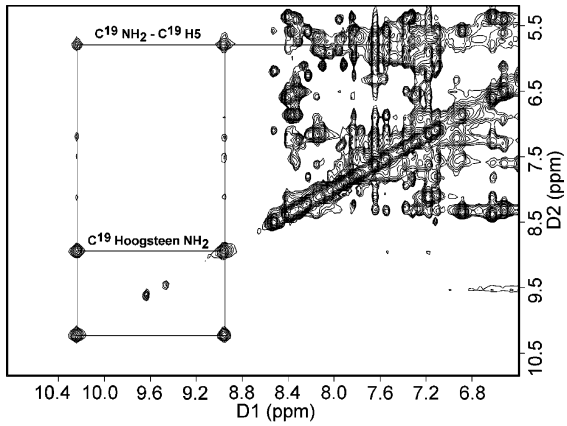

Figure 3. ^{1}H NOESY spectrum showing the assignment of the amino proton resonances of nucleotide C^{19} (complementary to X^6) following its H5 proton resonance. These resonances are observed at $\delta \sim 10.22$ and $\delta \sim 8.95$ ppm. The downfield chemical shifts of the C^{19} amino protons are characteristic of Hoogsteen pairing at X^6•C^{20}.

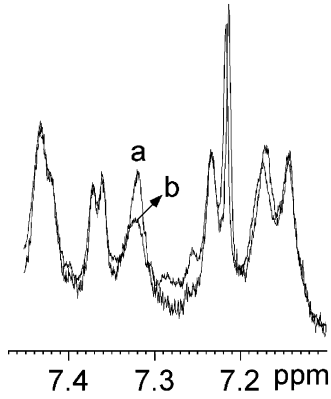

Figure 4. Superposition of ^{1}H NMR spectra of the 1,N^2-ϵdG-modified duplex (curve a) and after selective deuteration of the 1,N^2-ϵdG H7 proton (curve b). The experiments were conducted at pH 5.2 and 7 °C.

overlap of the H6 and H7 protons was reduced by one-half. A similar superposition of the etheno resonances was observed for the 1,N^6-ethenodeoxyadenosine (1,N^6-ϵdA) (*syn*)•dG(*anti*) base pair in duplex DNA, in which both of the etheno protons were superpositioned at 7.48 ppm (*41*). A strong NOE was observed between the overlapped X^6 H6 and H7 resonances and the T^5 CH_3 (Figure 5A, peak a). The X^6 overlapped X^6 H6 and H7 resonances showed a NOE to T^5 H6 (Figure 5A, peak c). A weak cross-strand NOE was observed between the overlapped X^6 H6 and H7 resonances and the T^{17} CH_3 (Figure 5A, peak c). Two additional cross-peaks (Figure 5A, peak d and e) were observed. These were also detected in the 70 ms mixing time NOESY spectrum (Figure 5B, peaks d and e), at the same intensity as was observed in the 250 ms mixing time data. Accordingly, these two cross-peaks were assigned as arising from conformational exchange. This conformational exchange was attributed to the *syn*/*anti* rotation of the glycosyl bond on the NMR time scale, since the chemical shifts of the two exchange peaks were comparable to the chemical shifts observed for the *anti* conformation of the 1,N^2-ϵdG etheno protons at pH 8.6 in the 5′-TXG-3′ sequence context (*32*).

4. Chemical Shift Perturbations. Comparison of the modified duplex with the corresponding unmodified duplex suggested that at pH 5.2 1,N^2-ϵdG introduced a localized structural perturbation into the duplex DNA (Figure 6). Differences were observed at the adducted base pair X^6•C^{19} and extended to its 5′-neighbor base pair T^5•A^{20} and 3′-neighbor base pair G^7•C^{18}.

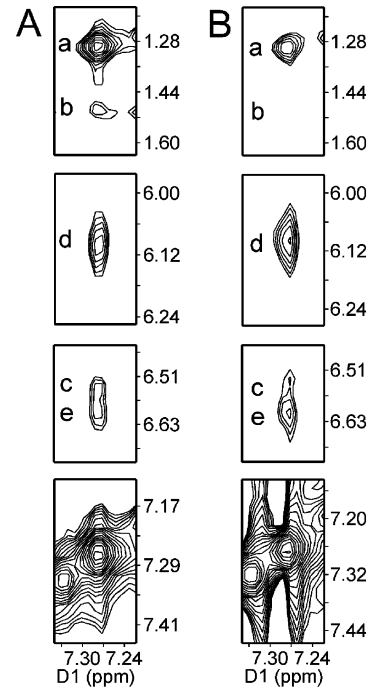

Figure 5. ^{1}H NOESY spectrum (tile plot) showing the assignment of the exocyclic etheno protons H7 and H6 and NOEs between the etheno and the DNA protons. (A and B) The NOESY spectra recorded at 250 and 70 ms mixing times. Cross-peaks: a, X^6 H6/H7→T^5 CH_3; b, X^6 H6/H7→T^{17} CH_3; c, X^6 H7/H6→T^5 H6; d, conformational exchange peak from X^6 H6; and e, conformation exchange peak from X^6 H7. The spectrum was recorded at 7 °C (pH 5.2).

The major change was observed for X^6 H2, which shifted upfield 0.6 ppm as compared to G^6 H8 in the unmodified duplex. The X^6 H1′ resonance shifted downfield by 0.3 ppm, while the X^6 H2′ resonance shifted upfield by 0.5 ppm. The complementary C^{19} H1′ and H2′ resonances shifted upfield 0.3 and 0.6 ppm, respectively. The T^5 H6 resonance shifted upfield by 0.5 ppm, while the T5 H2″ resonance shifted downfield by 0.3 ppm. The C^{18} H6 and A^{20} H8 protons showed 0.1 and 0.2 ppm downfield shifts, respectively.

Observation of a Second Conformational Equilibrium Involving the 3′-Neighbor G^7•C^{18}. Two additional weak signals were observed in the 9−11 ppm region of the NOESY spectrum (Figure 2A). These were attributed to a second conformational equilibrium allowing the formation of tandem Hoogsteen pairs, at base pair X^6•C^{19} and the 3′-neighbor base C^{18}. This conclusion was supported by the observation of a second small peak in very far downfield region of the spectrum, assigned as the protonated C^{18} imine. The broadening of the G^7 N1H imino resonance suggested that base pair G^7•C^{18} equilibrated between the Watson−Crick and the Hoogsteen pairing arrangements, with the Watson−Crick pair favored at pH 5.2. The absence of NOEs between the G^7 N1H imino proton and the amino protons of the complementary C^{18} (Figure 2B) also suggested that the two conformations existed in intermediate exchange on the NMR time scale. This was consistent with the absence of the G^7 H8→G^7 H1′ NOE, the broadening of the X^6 H1′→G^7 H8 NOE cross-peak, and the absence of the G^7 H1′→A^8 H8 NOE.

Molecular Modeling. The observation that the 3′-neighbor G^7•C^{18} base pair was simultaneously equilibrating between the *syn* and *anti* conformations led to the conclusion that at pH 5.2, the 1,N^2-ϵdG-adducted duplex existed as a mixture of species, with one species involving formation of a Hoogsteen pair at X^6•C^{19} and the second conformational equilibrium allowing formation of tandem Hoogsteen pairs at X^6•C^{19} and

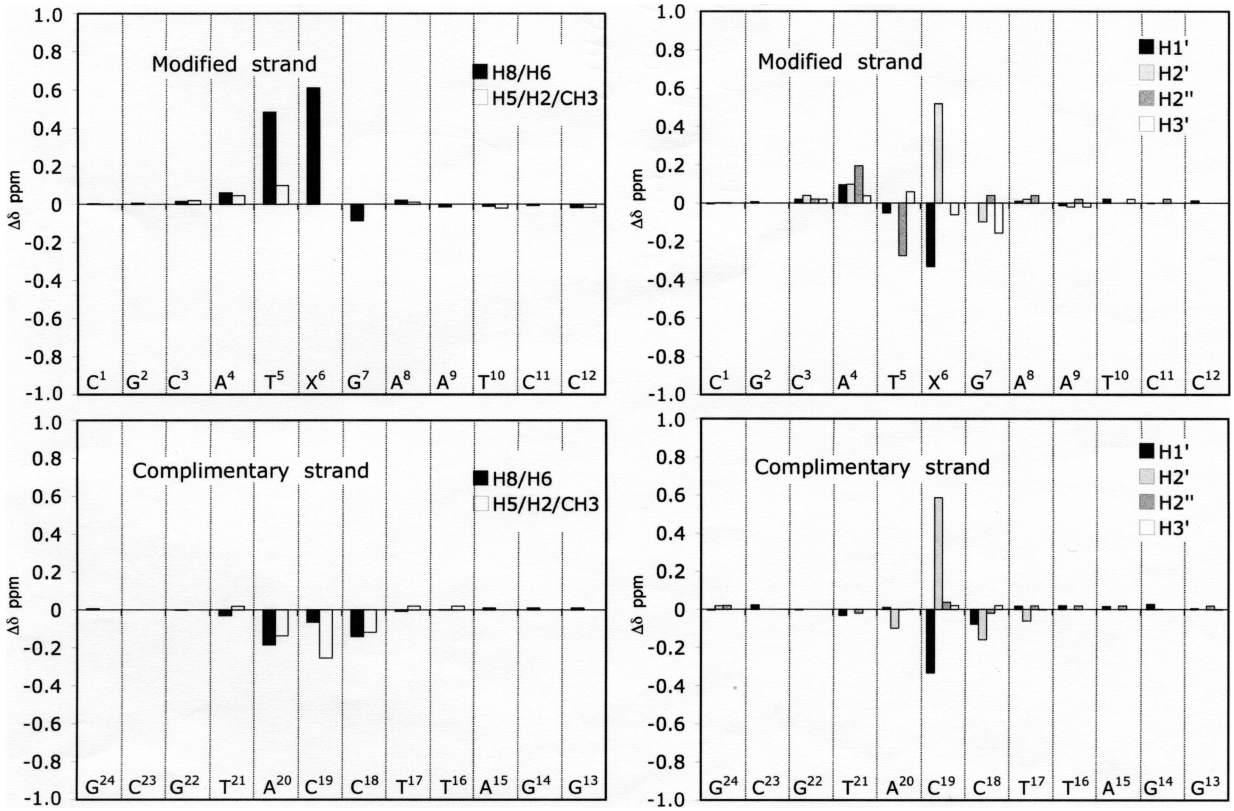

Figure 6. Chemical shift differences observed for 1,N^2-ϵdG-modified duplex as compared to the corresponding unmodified duplex at pH 5.2. $\Delta\delta = [\delta_{\text{unmodified oligodeoxynucleotide}} - \delta_{\text{modified oligodeoxynucleotide}}]$ (ppm).

G^7•C^{18} (Figure 7). The interconversion of these two conformational equilibria at an intermediate rate on the NMR time scale, evidenced by the broadening and loss of key NOEs, precluded the determination of a refined structure of the 1,N^2-ϵdG adduct at pH 5.2. Instead, potential energy-minimized structures for the major species present at equilibrium, involving a Hoogsteen X^6•C^{19} base pair and a Watson−Crick G^7•C^{18} base pair (Figure 7A), and a minor species, involving tandem X^6•C^{19} and G^7•C^{18} Hoogsteen base pairs (Figure 7B), were calculated. For the major species, X^6 was rotated ~180° about the glycosyl bond into the *syn* conformation. For the minor species, both X^6 and G^7 were rotated ~180° about the glycosyl bonds. These starting structures were potential energy minimized using 100 iterations of conjugate gradients minimization to relieve poor van der Waals contacts. Watson−Crick hydrogen-bonding restraints were applied at all of the base pairs with the exception of X^6•C^{19} in the major species and X^6•C^{19} and G^7•C^{18} in the minor species, for which Hoogsteen base pair restraints were used. The restraints were justified by data that showed imino and amino proton resonances consistent with a right-handed Watson−Crick paired duplex except at base pairs X^6•C^{19} and G^7•C^{18}, with formation of Hoogsteen pairs at these two sites. No deoxyribose pseudorotation or backbone torsion angle restraints were used for the X^6•C^{19} and G^7•C^{18} base pairs. Five hundred cycles of potential energy minimization using the conjugate gradients algorithm were applied.

The molecular modeling of these two species indicated that for the major species (Figure 7A), the Hoogsteen X^6•C^{19} and Watson−Crick G^7•C^{18} base pairs, could be accommodated within the DNA duplex with minimal distortion. The 1,N^2-ϵdG etheno protons faced into the major groove, whereas the imidazole H2 proton of the modified guanosine faced into the minor groove. In the minor species (Figure 7B), the formation of tandem X^6•C^{19} and G^7•C^{18} Hoogsteen base pairs was also accommodated within the DNA duplex with minimal disruption.

Figure 8 details the possible stacking interactions in the two species, on the basis of the potential energy minimization calculations. The stacking of T^5 above the Hoogsteen conformation of modified base pair X^6•C^{19} was consistent with the observation of NOEs between overlapped X^6 H7 and H6 resonances and T^5 CH_3 and T^5 H6 (Figure 5). The proximity of the imidazole proton of 1,N^2-ϵdG to the A^{20} H2 proton, due to the Hoogsteen conformation of base pair X^6•C^{19}, resulting in observation of an NOE cross-peak at 7.12 ppm (Figure 1), is evident. In the minor species involving the tandem Hoogsteen pairing arrangement, the two guanosine bases formed a partial stacking arrangement, and likewise, the two cytosine bases formed a partial stacking arrangement.

Discussion

The 1,N^2-ϵdG adduct is of interest because etheno DNA adducts (*1*) arise both from exogenous exposures to vinyl halides and other vinyl monomers (*2–9*) and also as a consequence of endogenous exposure to lipid peroxidation products (*9, 42, 43*). The exocyclic ring masks the Watson−Crick base pair coding face of dG and presents a sterically bulky lesion. In this duplex pH 8.6, the 1,N^2-ϵdG adduct adopts the *anti* conformation about the glycosyl bond (*32*). In the present study, the solution structure of 1,N^2-ϵdG adduct placed in the same sequence and opposite to cytosine is reported at pH 5.2.

Structure of 1,N^2-ϵdG in the 5′-TXG-3′ Sequence Context at pH 5.2. At pH 5.2, 1,N^2-ϵdG adopts the *syn* conformation about the glycosyl bond in the 5′-TXG-3′ sequence context. The distinguishing feature is the Hoogsteen pair at the lesion site X^6•C^{19}. The observation of a strong NOE between

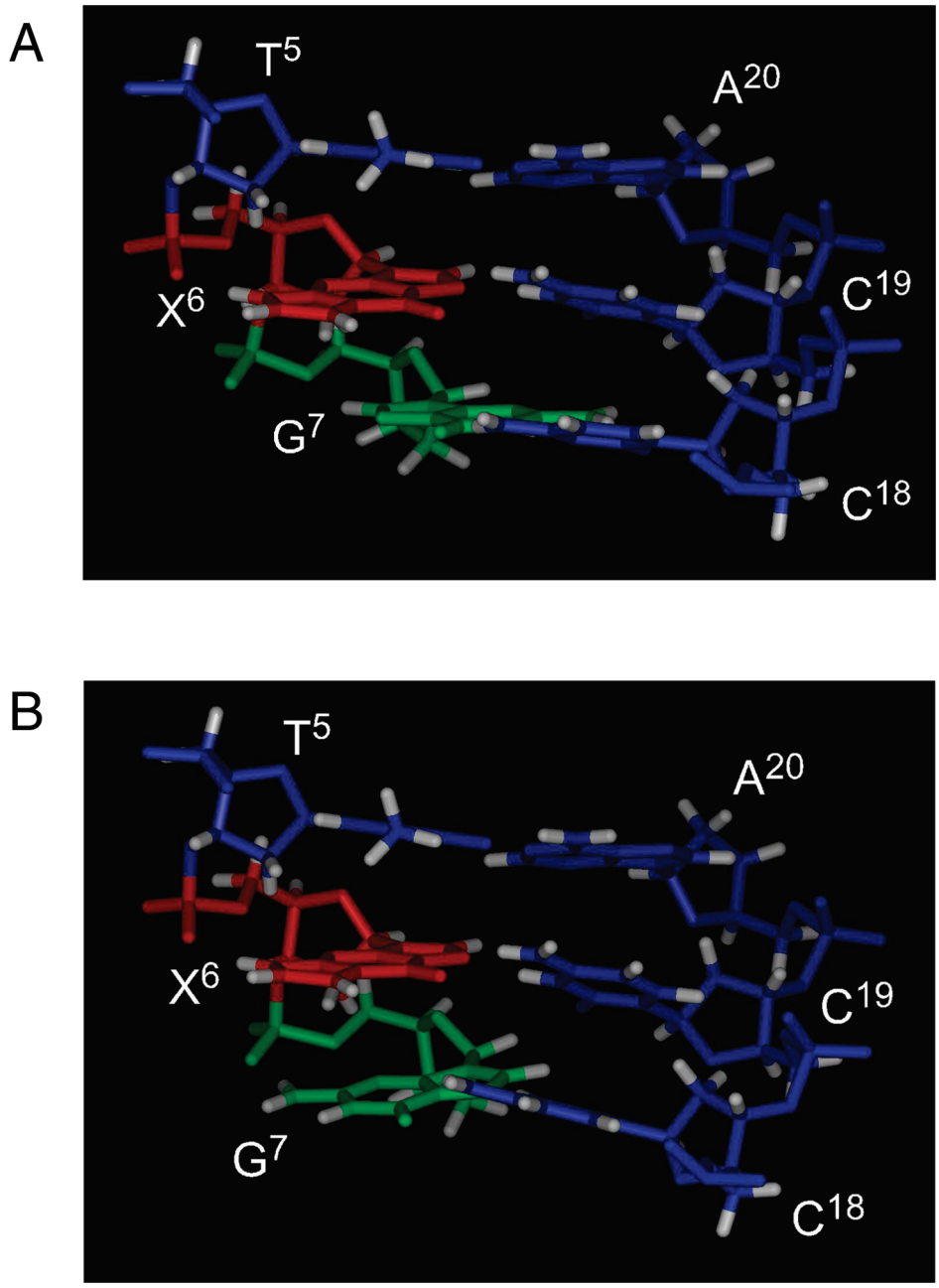

Figure 7. Molecular models of the central segment 5′-TXG-3′•5′-CCA-3′ of the 1,N^2-ϵdG-modified duplex derived from potential energy minimization. (A) In the first conformation, X^6 and G^7 are colored in red and green, respectively. Base pair X^6•C^{19} is in the Hoogsteen conformation, and the 5′- and 3′-neighbor base pairs are in the Watson−Crick conformations. (B) In the second conformation, X^6 and G^7 are colored in red and green, respectively. Base pairs X^6•C^{19} and G^7•C^{18} are both in the Hoogsteen conformation. In both conformations, the X^6 etheno protons face into the major groove, and the structural perturbation of the DNA helix is localized.

X^6 H2 and X^6 H1′, observed in the NOESY spectrum recorded at a mixing time of 70 ms, indicative of close contact between these protons, establishes that the glycosyl torsion angle of the 1,N^2-ϵdG nucleotide is in the *syn* conformation (Figure 1B). This orients the exocyclic etheno protons into the major groove. Accordingly, a strong NOE is observed between T^5 CH_3 and X^6 H6 and H7 (Figure 5A, peak a). The X^6 H6 and H7 protons exhibit NOEs to T^5 H6 (Figure 5A, peak c). A weak cross-strand NOE is observed between X^6 H6 and H7 and T^{17} CH_3 (Figure 5A, peak b). The absence of additional NOEs between the 1,N^2-ϵG H6 and H7 protons and the DNA protons is attributed to the placement of 1,N^2-ϵG etheno protons in the major groove. The *syn* conformation of the glycosyl bond is also reflected in the chemical shift of the imidazole proton X^6 H2, which resonates at a higher field at pH 5.2 (Tables 1) as a consequence of placement of X^6 H2 in the center of the helix and its stacking between the neighboring base pairs. In the complementary strand, the A^{20} H2 resonance provides a marker for monitoring the conformational change from the X^6(*anti*)•C^{19}(*anti*) alignment at basic pH to the X^6(*syn*)•C^{19}(*anti*) alignment at acidic pH. At pH 5.2, a strong NOE is observed between A^{20} H2 and X^6 H2. This is not observed at pH 8.6 (*32*) because the distance between these protons is more than 6 Å when 1,N^2-ϵdG adopts the *anti* conformation about the glycosyl bond. The exchange peaks between the superimposed 1,N^2-ϵdG H6 and H7 protons, located at 7.3 ppm at pH 5.2, and the resonances located at 6.1 and 6.6 ppm (Figure 5A, peaks d and e) also provide markers for monitoring the conformational change from the X^6(*anti*)•C^{19}(*anti*) alignment at basic pH to the X^6(*syn*)•C^{19}(*anti*) alignment at acidic pH. The etheno H6 and

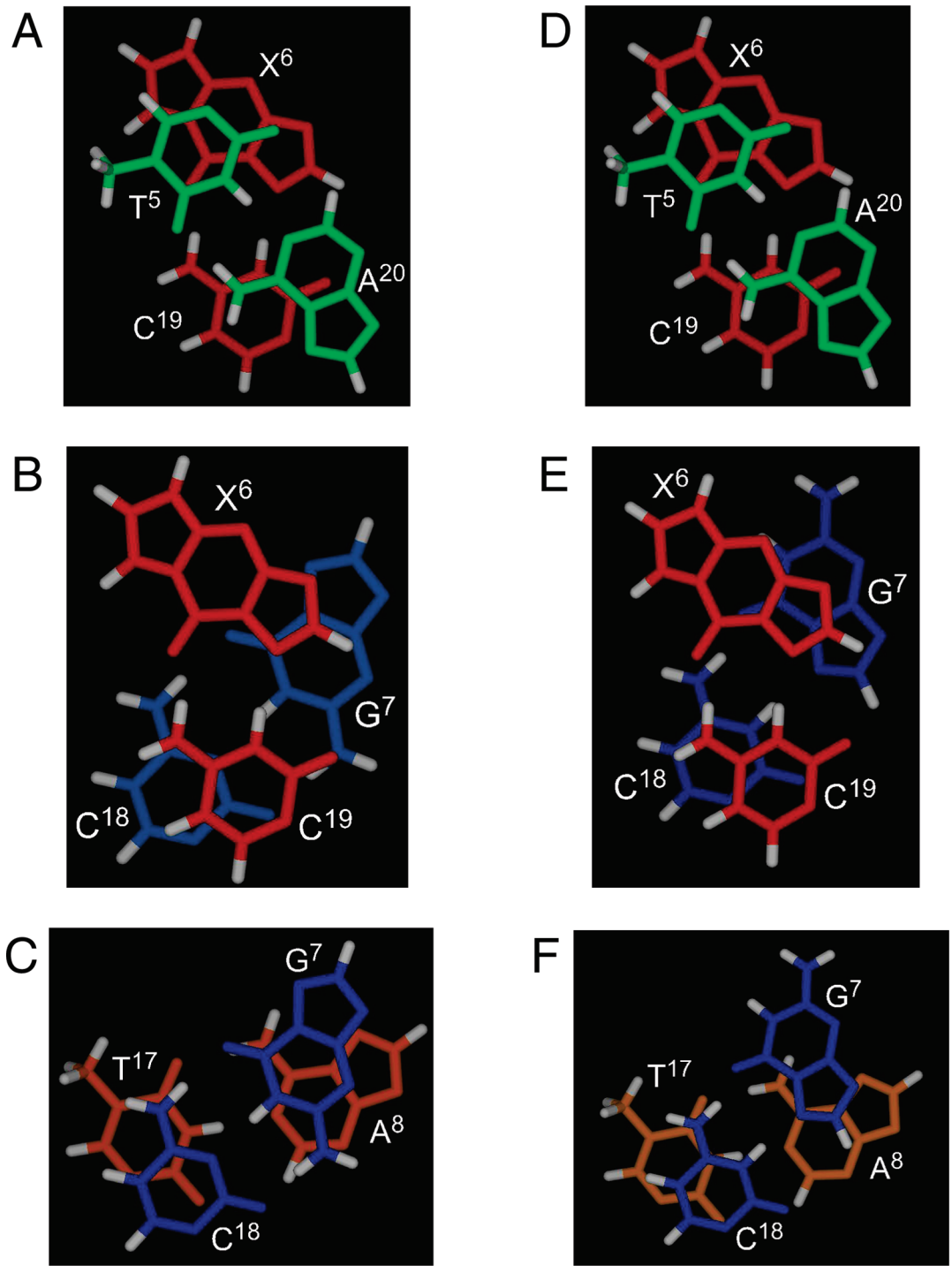

Figure 8. Molecular models of the base stacking of the 1,N^2-ϵdG adduct. (A) The first conformation. Stacking of base pairs T^5•A^{20} (green) and X^6•C^{19} (red). (B) The first conformation. Stacking of base pairs X^6•C^{19} (red) and G^7•C^{18} (blue). (C) The first conformation. Stacking of base pairs G^7•C^{18} (blue) and A^8•T^{17} (orange). (D) The second conformation. Stacking of base pairs T^5•A^{20} (green) and X^6•C^{19} (red). (E) The second conformation. Stacking of base pairs X^6•C^{19} (red) and G^7•C^{18} (blue). (F) The second conformation. Stacking of base pairs G^7•C^{18} (blue) and A^8•T^{17} (orange).

H7 protons resonated at 6.5 and 6.2 ppm, respectively, when 1,N^2-ϵdG adopted the *anti* conformation at basic pH (*32*).

The *syn* orientation of 1,N^2-ϵdG glycosyl bond facilitates protonation of the complementary cytosine, allowing formation of a Hoogsteen pair. This is consistent with the downfield shift of the C^{19} amino protons, characteristic of a protonated cytosine (*44*) involved in a Hoogsteen base pair (*45*). The farthest downfield-shifted amino proton, assigned as the hydrogen-bonded amine proton at C^{19}, exhibits an NOE to C^{19} H5, but no NOE to a guanine imino proton, consistent with the formation of a Hoogsteen, as opposed to a Watson−Crick pair (Figure 3). The presence of the Hoogsteen pair is corroborated by the observation of a resonance in the very far downfield region of the spectrum, attributed to the protonated cytosine imine in the X^6•C^{19} Hoogsteen pair. The latter resonance is weak, attributed to exchange with solvent, precluding observation of an NOE to the hydrogen-bonded C^{19} amino proton. The *syn* glycosyl conformation at X^6 placed the X^6 H5 amino proton near the backbone and exposed to solvent exchange, which was consistent with the failure to observe it.

The chemical shift perturbations of the aromatic and anomeric protons in going from the unmodified oligodeoxynucleotide to

Table 1. Comparison of Chemical Shift Differences[a] (ppm) for the 1,N^2-ϵdG-Adducted Duplex at pH 8.6 vs pH 5.2[b]

proton	T^5	X^6	G^7	C^{18}	C^{19}	A^{20}
H8/H6/H2[c]	0.51	0.82	0.04	0.01	0.07	−0.03
H1′	0.15	−0.59	*d*	0.14	0.44	0.09
H2′	*d*	0.3	0.1	0.11	0.39	0.01
H2″	−0.33	*d*	0.13	−0.06	−0.08	0.08
H3′	0.08	−0.14	−0.1	0.11	−0.02	0.06
CH_3/H2	0.21					−0.24
N1H/N3H/N^4H	0.06		−0.34	−0.28, −0.17	*d*	

[a] δ (pH 8.6) − δ (pH 5.2). [b] Positive and negative values correspond to downfield and upfield chemical shifts, respectively, on proceeding from pH 5.2 to pH 8.6. [c] Imidazole proton of X^6. [d] The corresponding proton resonances were not detected in the 1,N^2-ϵdG duplex at 7 °C (pH 8.6).

the X^6 (*syn*)•C^{19} (*anti*) Hoogsteen conformation, at pH 5.2, suggest that the influence of the 1,N^2-ϵdG base is localized to the site of adduction and the neighboring base pairs. These chemical shift changes are the result of base stacking and electrostatic changes caused by the rotation of the 1,N^2-ϵdG adduct into the *syn* conformation and formation of the X^6•C^{19} Hoogsteen base pair. The upfield chemical shifts of 0.6 and 0.33 ppm, respectively, for the X^6 H2 and H1′ resonances of the X^6•C^{19} base pair are consistent with formation of a Hoogsteen pair. Also, the complementary C^{19} H2′ resonance shifts upfield by 0.6 ppm and the C^{19} H1′ proton shifts downfield by 0.33 ppm. The upfield of X^6 H2 proton is characteristic of the *syn* conformation at this nucleotide. The upfield shift of the T^5 H1′ proton resonance is attributed to shielding arising from the aromatic ring of the 1,N^2-ϵdG moiety in the *syn* conformation about the glycosyl bond. The broadening of A^4 H1′→T^5 H6 and T^5 H6→T^5 H1′ NOEs suggests that the 5′-neighboring T^5•A^{20} base pair is also somewhat perturbed in the 5′-TXG-3′ sequence at pH 5.2. The chemical shifts of the proton resonances for T^5 H6, C^{18} H6, C^{18} H5, A^{20} H8, A^{20} H2, T^5 H1′, and C^{18} H2′ suggest that 1,N^2-ϵdG induces a significant structural perturbation involving its immediate neighboring base pairs.

Second Conformational Equilibrium of the 1,N^2-ϵdG Adduct in the 5′-TXG-3′ Sequence at pH 5.2. Upon lowering the pH of the 1,N^2-ϵdG-adducted duplex to 5.2, the presence of a second equilibrium involving the 3′-neighbor base pair G^7•C^{18} becomes apparent. This leads to the spectroscopic appearance of a second species involving the formation of tandem Hoogsteen pairs, at base pair X^6•C^{19} and the 3′-neighbor base C^{18}. This is supported by the observation of a small peak in the far downfield region of the spectrum, assigned as the protonated C^{18} imine. The broadening of the G^7 N1H imino resonance suggests that base pair G^7•C^{18} equilibrates between Watson−Crick and Hoogsteen pairing. The absence of NOEs between the G^7 N1H imino proton and the amino protons of the complementary C^{18} (Figure 3) suggests that the two species exist in intermediate exchange on the NMR time scale. This is consistent with the absence of the G^7 H8→G^7 H1′ NOE, the broadening of the X^6 H1′→G^7 H8 NOE cross-peak, and the absence of the G^7 H1′→A^8 H8 NOE.

Comparison with the 1,N^2-ϵdG:dC Base Pair in the 5′-CXC-3′ Sequence Context. Zaliznyak et al. (*31*) reported the structure of DNA containing the 1,N^2-ϵdG adduct paired to dC at pH 6.9, in the 5′-CXC-3′ sequence context. In contrast to the present results obtained at pH 5.2 and previous results obtained at pH 8.6 in the 5′-TXG-3′ sequence (*32*), their data suggested a minimally perturbed duplex structure at neutral pH in the 5′-CXC-3′ sequence. The 1,N^2-ϵdG adduct remained in the *anti* conformation about the glycosyl bond and was embedded inside the helix and stacked between the flanking base pairs. One significant difference with respect to the present and previous (*32*) results in the 5′-TXG-3′ sequence was that in the 5′-CXC-3′ sequence, the lesion partner dC was extrahelical but was located in the minor groove of the duplex, potentially forming a hydrogen bond with the sugar O4′ atom of a nucleotide two bp away (*31*). The presently observed NOEs between the 1,N^2-ϵdG•C base pair and the DNA clearly do not support a minor groove orientation of the opposing cytosine for the 5′-TXG-3′ sequence. The minor groove of DNA is relatively proton-dense. Modeling studies in which the opposing cytosine was placed in the minor groove, in an orientation similar to the Zaliznyak et al. (*31*) structure in the 5′-CXC-3′ sequence, predicted that several anticipated NOEs were the opposing cytosine located in the minor groove. These were not observed. Likewise, close inspection of previously reported NMR data for the 1,N^2-ϵdG adduct at pH 8.6 in the 5′-TXG-3′ sequence (*32*) also does not support a minor groove orientation of the opposing cytosine. Thus, we conclude that the minor groove orientation of the opposing cytosine reported by Zaliznyak et al. (*31*) in the 5′-CXC-3′ sequence might be attributed to a sequence-specific conformational effect warranting further study. Zaliznyak et al. (*31*) also reported, similar to the present observations in the 5′-TXG-3′ sequence, that acidification resulted in the appearance of a second conformational equilibrium, involving protonation of the lesion partner dC and possible formation of a Hoogsteen-like base pair.

Comparison with 1,N^2-Propano-2′-deoxyguanosine (1,N^2-PdG). The present results are reminiscent of studies with 1,N^2-PdG, containing a six-member exocyclic ring, vs the five-member exocyclic ring in 1,N^2-ϵdG (*45, 46*). At acidic pH, 1,N^2-PdG forms a Hoogsteen pair with the complementary cytosine in the sequences 5′-TXT-3′•5′-ACA-3′ and 5′-CXC-3′•5′-GCG-3′ (X = PdG). In the latter sequence, both the modified base pair and its 3′-neighbor C•G base pair are disturbed. The 3′-neighbor base pair interconverts between Watson−Crick and Hoogsteen pairing. For 1,N^2-PdG, the conformational equilibrium at the 3′-neighbor base pair is sequence-dependent. In the 5′-TXT-3′ sequence, only the 1,N^2-PdG-modified base pair interconverts between Watson−Crick and Hoogsteen pairing; the 3′-neighbor base pair remains in the Watson−Crick conformation. A similar sequence-dependent effect may occur for 1,N^2-ϵdG.

Structure−Activity Relationships. When combined with previous work at pH 8.6 (*32*), the present results lead to the conclusion that when placed into the 5′-TXG-3′ sequence context at neutral pH, 1,N^2-ϵdG interconverts on the millisecond time scale between the *anti* and *syn* conformations of the glycosyl bond. Additionally, small amounts of a species involving tandem Hoogsteen pairs may be present. These conformational equilibria involving base pairs X^6•C^{19} and G^7•C^{18} may be relevant with regard to the recognition of 1,N^2-ϵdG by DNA glycosylases. The *E. coli* mismatch-specific uracil-DNA glycosylase and the human alkylpurine-DNA-*N*-glycosylase both release 1,N^2-ϵdG from DNA (*47*). Likewise, in mammalian cells, the alkylpurine-DNA-*N*-glycosylase repairs 1,N^6-ϵdA (*48*), whereas mismatch-specific thymine DNA glycosylase repairs 3,N^4-ethenodeoxycytosine (3,N^4-ϵdC) (*49*). The "flipping" of damaged nucleotides out of the DNA helix and into active site binding pockets provides a mechanism by which glycosylases interact with damaged DNA (for a review, see ref *50*). The 14 °C decrease in T_m of the 1,N^2-ϵdG-modified duplex, in combination with the conformational exchange in DNA at neutral pH, may facilitate damage recognition, for example, by human alkylpurine-DNA-*N*-glycosylase (*47*).

1,N^2-ϵdG-Modified Primer−Template Complexes with the *Sulfolobus solfataricus* DNA Polymerase (Dpo4). The insertion of the 1,N^2-ϵdG lesion into a template containing the 5′-TXG-3′ sequence and the formation of either binary or ternary complexes with the *S. solfataricus* DNA polymerase Dpo4 were reported by Zang et al. (*29*). In each of these complexes, 1,N^2-ϵdG adopts the *anti* conformation about the glycosyl bond (*29*). Thus, whereas at neutral pH when placed opposite dC in duplex DNA, a mixture of Hoogsteen and Watson−Crick pairing interactions is observed for 1,N^2-ϵdG, in these complexes, the Dpo4 polymerase selects for the *anti* conformation about the glycosyl bond. When primer extension was done by the Dpo4 polymerase in the presence of a mixture of all four dNTPs, product analysis led to the conclusion that this enzyme uses several mechanisms, including dATP incorporation opposite 1,N^2-ϵdG and also a variation of dNTP-stabilized misalignment, to generate both base pair substitution and frameshift mutations (*29*). The insertion of 1,N^2-PdG into a template and the subsequent formation of ternary complexes with the Dpo4 polymerase has been recently reported (*51*). Like 1,N^2-ϵdG, 1,N^2-PdG also adopts the *anti* conformation about the glycosyl bond in these complexes, supporting the notion that the Dpo4 polymerase selects for the *anti* conformation of 1,N^2-ϵdG exocyclic adducts. On the other hand, the Dpo4 polymerase successfully inserts dCTP opposite 1,N^2-ϵdG approximately 20% of the time (*29*). The *syn* conformation of 1,N^2-ϵdG potentially allows Hoogsteen pairing with incoming dCTP, which might facilitate error-free polymerase bypass. Obtaining structures of 1,N^2-ϵdG in complex with different human bypass polymerases will be of future interest in delineating specific mechanisms by which 1,N^2-ϵdG induces mutations in DNA.

Summary

At neutral pH, 1,N^2-ϵdG exists as a blend of conformations in the 5′-TXG-3′ sequence context in duplex DNA. These involve interconversion of the glycosyl bond between the *anti* and the *syn* conformations. Increasing the pH to 8.6 shifts the equilibrium predominantly toward the *anti* conformation (*32*), whereas decreasing the pH to 5.2 shifts the equilibrium predominantly toward the *syn* conformation and the formation of a Hoogsteen pair at X^6•C^{19}. At the lower pH, a second species becomes apparent, involving the formation of tandem Hoogsteen pairs at X^6•C^{19} and G^7•C^{18}.

Acknowledgment. Markus Voehler assisted with the collection of NMR data. This work was supported by NIH Grants PO1 ES05355 (C.J.R. and M.P.S.) and RO1 ES10375 (F.P.G.). Funding for NMR was supplied by Vanderbilt University, the Vanderbilt Center in Molecular Toxicology, P30 ES00267, and by NIH Grant RR05805. The Vanderbilt Ingram Cancer Center is supported by NIH Grant P30 CA68485.

Supporting Information Available: Table S1, chemical shifts of nonexchangeable protons for the unmodified duplex at pH 5.2; Table S2, chemical shifts of nonexchangeable protons for the 1,N^2-ϵdG-modified duplex at pH 5.2; Table S3, chemical shifts of exchangeable protons for the 1,N^2-ϵdG-modified duplex at pH 5.2; Table S4, chemical shifts of exchangeable protons for the unmodified duplex at pH 5.2; Figure S1, NOESY data showing cross-peaks between the base protons and the deoxyribose H2′ and H2″ protons at pH 5.2; Figure S2, NOESY data showing cross-peaks between the base aromatic and the deoxyribose H1′ protons in the 5′→3′ direction for the unmodified duplex at pH 5.2; Figure S3; NOESY data showing cross-peaks between the C^{19} amino protons and the Watson−Crick hydrogen-bonded imino proton of the 5′-neighbor T^5•A^{20} base pair; and Figure S4, chemical shift differences observed for 1,N^2-ϵdG-modified duplex as compared to the corresponding unmodified duplex at pH 5.2: $\Delta\delta = [\delta_{\text{unmodified oligodeoxynucleotide}} - \delta_{\text{modified oligodeoxynucleotide}}]$ (ppm). This material is available free of charge via the Internet at http://pubs.acs.org.

References

(1) Barbin, A. (2000) Etheno-adduct-forming chemicals: From mutagenicity testing to tumor mutation spectra. *Mutat. Res. 462*, 55–69.
(2) Barbin, A., Bresil, H., Croisy, A., Jacquignon, P., Malaveille, C., Montesano, R., and Bartsch, H. (1975) Liver-microsome-mediated formation of alkylating agents from vinyl bromide and vinyl chloride. *Biochem. Biophys. Res. Commun. 67*, 596–603.
(3) Green, T., and Hathway, D. E. (1978) Interactions of vinyl chloride with rat-liver DNA *in vivo*. *Chem.-Biol. Interact. 22*, 211–224.
(4) Eberle, G., Barbin, A., Laib, R. J., Ciroussel, F., Thomale, J., Bartsch, H., and Rajewsky, M. F. (1989) 1,N^6-etheno-2′-deoxyadenosine and 3,N^4-etheno-2′-deoxycytidine detected by monoclonal antibodies in lung and liver DNA of rats exposed to vinyl chloride. *Carcinogenesis 10*, 209–212.
(5) Fedtke, N., Boucheron, J. A., Walker, V. E., and Swenberg, J. A. (1990) Vinyl chloride-induced DNA adducts. II: Formation and persistence of 7-(2′-oxoethyl)guanine and N^2,3-ethenoguanine in rat tissue DNA. *Carcinogenesis 11*, 1287–1292.
(6) Guengerich, F. P., Mason, P. S., Stott, W. T., Fox, T. R., and Watanabe, P. G. (1981) Roles of 2-haloethylene oxides and 2-haloacetaldehydes derived from vinyl bromide and vinyl chloride in irreversible binding to protein and DNA. *Cancer Res. 41*, 4391–4398.
(7) Guengerich, F. P., and Kim, D. H. (1991) Enzymatic oxidation of ethyl carbamate to vinyl carbamate and its role as an intermediate in the formation of 1,N^6-ethenoadenosine. *Chem. Res. Toxicol. 4*, 413–421.
(8) Guengerich, F. P. (1992) Roles of the vinyl chloride oxidation products 1-chlorooxirane and 2-chloroacetaldehyde in the *in vitro* formation of etheno adducts of nucleic acid bases [corrected]. *Chem. Res. Toxicol. 5*, 2–5.
(9) Bartsch, H., Barbin, A., Marion, M. J., Nair, J., and Guichard, Y. (1994) Formation, detection, and role in carcinogenesis of ethenobases in DNA. *Drug. Metab. Rev. 26*, 349–371.
(10) Nair, U., Bartsch, H., and Nair, J. (2007) Lipid peroxidation-induced DNA damage in cancer-prone inflammatory diseases: A review of published adduct types and levels in humans. *Free Radical Biol. Med. 43*, 1109–1120.
(11) Lee, S. H., and Blair, I. A. (2000) Characterization of 4-oxo-2-nonenal as a novel product of lipid peroxidation. *Chem. Res. Toxicol. 13*, 698–702.
(12) Lee, S. H., Oe, T., and Blair, I. A. (2001) Vitamin C-induced decomposition of lipid hydroperoxides to endogenous genotoxins. *Science 292*, 2083–2086.
(13) Lee, S. H., Oe, T., and Blair, I. A. (2002) 4,5-Epoxy-2(*E*)-decenal-induced formation of 1N^6-etheno-2′-deoxyadenosine and 1,N^2-etheno-2′-deoxyguanosine adducts. *Chem. Res. Toxicol. 15*, 300–304.
(14) Lee, S. H., Arora, J. A., Oe, T., and Blair, I. A. (2005) 4-Hydroperoxy-2-nonenal-induced formation of 1,N^2-etheno-2′-deoxyguanosine adducts. *Chem. Res. Toxicol. 18*, 780–786.
(15) Kawai, Y., Uchida, K., and Osawa, T. (2004) 2′-Deoxycytidine in free nucleosides and double-stranded DNA as the major target of lipid peroxidation products. *Free Radical Biol. Med. 36*, 529–541.
(16) Lee, S. H., Silva Elipe, M. V., Arora, J. S., and Blair, I. A. (2005) Dioxododecenoic acid: A lipid hydroperoxide-derived bifunctional electrophile responsible for etheno DNA adduct formation. *Chem. Res. Toxicol. 18*, 566–578.
(17) Sattsangi, P. D., Leonard, N. J., and Frihart, C. R. (1977) 1,N^2-Ethenoguanine and N^2,3-ethenoguanine synthesis and comparison of electronic spectral properties of these linear and angular triheterocycles related to Y bases. *J. Org. Chem. 42*, 3292–3296.
(18) Guengerich, F. P., Persmark, M., and Humphreys, W. G. (1993) Formation of 1,N^2- and N^2,3-ethenoguanine derivatives from 2-halooxiranes: Isotopic labeling studies and formation of a hemiaminal derivative of N^2-(2-oxoethyl)guanine. *Chem. Res. Toxicol. 6*, 635–648.
(19) Guengerich, F. P., and Persmark, M. (1994) Mechanism of formation of ethenoguanine adducts from 2-haloacetaldehydes: ^{13}C-Labeling patterns with 2-bromoacetaldehyde. *Chem. Res. Toxicol. 7*, 205–208.
(20) Morinello, E. J., Ham, A. J., Ranasinghe, A., Sangaiah, R., and Swenberg, J. A. (2001) Simultaneous quantitation of N^2,3-ethenogua-

nine and 1,N^2-ethenoguanine with an immunoaffinity/gas chromatography/high-resolution mass spectrometry assay. *Chem. Res. Toxicol. 14*, 327–334.
(21) Marques, S. A., Loureiro, A. P., Gomes, O. F., Garcia, C. C., Di Mascio, P., and Medeiros, M. H. (2004) Induction of 1,N^2-etheno-2′-deoxyguanosine in DNA exposed to beta-carotene oxidation products. *FEBS Lett. 560*, 125–130.
(22) Kawai, Y., Kato, Y., Nakae, D., Kusuoka, O., Konishi, Y., Uchida, K., and Osawa, T. (2002) Immunohistochemical detection of a substituted 1,N^2-ethenodeoxyguanosine adduct by ω-6 polyunsaturated fatty acid hydroperoxides in the liver of rats fed a choline-deficient, l-amino acid-defined diet. *Carcinogenesis 23*, 485–489.
(23) Loureiro, A. P., Marques, S. A., Garcia, C. C., Di Mascio, P., and Medeiros, M. H. (2002) Development of an on-line liquid chromatography-electrospray tandem mass spectrometry assay to quantitatively determine 1,N^2-etheno-2′-deoxyguanosine in DNA. *Chem. Res. Toxicol. 15*, 1302–1308.
(24) Martinez, G. R., Loureiro, A. P., Marques, S. A., Miyamoto, S., Yamaguchi, L. F., Onuki, J., Almeida, E. A., Garcia, C. C., Barbosa, L. F., Medeiros, M. H., and Di Mascio, P. (2003) Oxidative and alkylating damage in DNA. *Mutat. Res. 544*, 115–127.
(25) Pang, B., Zhou, X., Yu, H., Dong, M., Taghizadeh, K., Wishnok, J. S., Tannenbaum, S. R., and Dedon, P. C. (2007) Lipid peroxidation dominates the chemistry of DNA adduct formation in a mouse model of inflammation. *Carcinogenesis 28*, 1807–1813.
(26) Langouet, S., Mican, A. N., Muller, M., Fink, S. P., Marnett, L. J., Muhle, S. A., and Guengerich, F. P. (1998) Misincorporation of nucleotides opposite five-membered exocyclic ring guanine derivatives by *Escherichia coli* polymerases in vitro and in vivo: 1,N^2-Ethenoguanine, 5,6,7,9-tetrahydro-9-oxoimidazo[1,2-α]purine, and 5,6,7,9-tetrahydro-7-hydroxy-9-oxoimidazo[1,2-α]purine [published erratum appears in *Biochemistry* (1998) *37* (24), 8816]. *Biochemistry 37*, 5184–5193.
(27) Akasaka, S., and Guengerich, F. P. (1999) Mutagenicity of site-specifically located 1,N^2-ethenoguanine in Chinese hamster ovary cell chromosomal DNA. *Chem. Res. Toxicol. 12*, 501–507.
(28) Langouet, S., Muller, M., and Guengerich, F. P. (1997) Misincorporation of dNTPs opposite 1,N^2-ethenoguanine and 5,6,7,9-tetrahydro-7-hydroxy-9-oxoimidazo[1,2-α]purine in oligonucleotides by *Escherichia coli* polymerases I *exo-* and II *exo-*, T7 polymerase *exo-*, human immunodeficiency virus-1 reverse transcriptase, and rat polymerase beta. *Biochemistry 36*, 6069–6079.
(29) Zang, H., Goodenough, A. K., Choi, J. Y., Irimia, A., Loukachevitch, L. V., Kozekov, I. D., Angel, K. C., Rizzo, C. J., Egli, M., and Guengerich, F. P. (2005) DNA adduct bypass polymerization by *Sulfolobus solfataricus* DNA polymerase Dpo4: Analysis and crystal structures of multiple base pair substitution and frameshift products with the adduct 1,N^2-ethenoguanine. *J. Biol. Chem. 280*, 29750–29764.
(30) Choi, J. Y., Zang, H., Angel, K. C., Kozekov, I. D., Goodenough, A. K., Rizzo, C. J., and Guengerich, F. P. (2006) Translesion synthesis across 1,N^2-ethenoguanine by human DNA polymerases. *Chem. Res. Toxicol. 19*, 879–886.
(31) Zaliznyak, T., Lukin, M., Johnson, F., and de Los Santos, C. (2008) Solution structure of duplex DNA containing the mutagenic lesion 1,N^2-etheno-2′-deoxyguanine. *Biochemistry* 4606–4613.
(32) Shanmugam, G., Goodenough, A. K., Kozekov, I. D., Guengerich, F. P., Rizzo, C. J., and Stone, M. P. (2007) Structure of the 1,N^2-etheno-2′-deoxyguanosine adduct in duplex DNA at pH 8.6. *Chem. Res. Toxicol. 20*, 1601–1611.
(33) Goodenough, A. K., Kozekov, I. D., Zang, H., Choi, J. Y., Guengerich, F. P., Harris, T. M., and Rizzo, C. J. (2005) Site specific synthesis and polymerase bypass of oligonucleotides containing a 6-hydroxy-3,5,6,7-tetrahydro-9H-imidazo[1,2-α]purin-9one base, an intermediate in the formation of 1,N^2-etheno-2′-deoxyguanosine. *Chem. Res. Toxicol. 18*, 1701–1714.
(34) Piotto, M., Saudek, V., and Sklenar, V. (1992) Gradient-tailored excitation for single-quantum NMR spectroscopy of aqueous solutions. *J. Biomol. NMR 2*, 661–665.
(35) Brunger, A. T. (1990) Refinement of three-dimensional structures of proteins and nucleic acids. In *Molecular Dynamics* (Goodfellow, J. M., Ed.) pp 137−178, CRC Press, Boca Raton.
(36) Arnott, S., and Hukins, D. W. L. (1972) Optimised parameters for A-DNA and B-DNA. *Biochem. Biophys. Res. Commun. 47*, 1504–1509.
(37) Frisch, M. J., *GAUSSIAN 98*, A. Gaussian, Inc., Pittsburgh, PA, 1998.
(38) Wang, J., Wang, W., Kollman, P. A., and Case, D. A. (2006) Automatic atom type and bond type perception in molecular mechanical calculations. *J. Mol. Graphics Modell. 25*, 247–260.
(39) Cullinan, D., Korobka, A., Grollman, A. P., Patel, D. J., Eisenberg, M., and de los Santos, C. (1996) NMR solution structure of an oligodeoxynucleotide duplex containing the exocyclic lesion 3,N^4-etheno-2′-deoxycytidine opposite thymidine: Comparison with the duplex containing deoxyadenosine opposite the adduct. *Biochemistry 35*, 13319–13327.
(40) Korobka, A., Cullinan, D., Cosman, M., Grollman, A. P., Patel, D. J., Eisenberg, M., and de los Santos, C. (1996) Solution structure of an oligodeoxynucleotide duplex containing the exocyclic lesion 3,N^4-etheno-2′-deoxycytidine opposite 2′- deoxyadenosine, determined by NMR spectroscopy and restrained molecular dynamics. *Biochemistry 5*, 13310–13318.
(41) de los Santos, C., Kouchakdjian, M., Yarema, K., Basu, A., Essigmann, J., and Patel, D. J. (1991) NMR studies of the exocyclic 1,N^6-ethenodeoxyadenosine adduct (ϵ dA) opposite deoxyguanosine in a DNA duplex. ϵ dA(syn):dG(anti) pairing at the lesion site. *Biochemistry 30*, 1828–1835.
(42) Nair, J., Barbin, A., Guichard, Y., and Bartsch, H. (1995) 1,N^6-Ethenodeoxyadenosine and 3,N^4-ethenodeoxycytine in liver DNA from humans and untreated rodents detected by immunoaffinity/^{32}P-postlabeling. *Carcinogenesis 16*, 613–617.
(43) Guichard, Y., el Ghissassi, F., Nair, J., Bartsch, H., and Barbin, A. (1996) Formation and accumulation of DNA ethenobases in adult Sprague-Dawley rats exposed to vinyl chloride. *Carcinogenesis 17*, 1553–1559.
(44) Kouchakdjian, M., Marinelli, E., Gao, X., Johnson, F., Grollman, A., and Patel, D. (1989) NMR studies of exocyclic 1,N^2-propanodeoxyguanosine adducts (X) opposite purines in DNA duplexes: Protonated X(*syn*):A(*anti*) pairing (acidic pH) and X(*syn*):G(*anti*) pairing (neutral pH) at the lesion site. *Biochemistry 28*, 5647–5657.
(45) Singh, U. S., Moe, J. G., Reddy, G. R., Weisenseel, J. P., Marnett, L. J., and Stone, M. P. (1993) ^{1}H NMR of an oligodeoxynucleotide containing a propanodeoxyguanosine adduct positioned in a $(CG)_3$ frameshift hotspot of *Salmonella typhimurium hisD3052*: Hoogsteen base-pairing at pH 5.8. *Chem. Res. Toxicol. 6*, 825–836.
(46) Weisenseel, J. P., Reddy, G. R., Marnett, L. J., and Stone, M. P. (2002) Structure of an oligodeoxynucleotide containing a 1,N^2-propanodeoxyguanosine adduct positioned in a palindrome derived from the *Salmonella typhimurium* hisD3052 gene: Hoogsteen pairing at pH 5.2. *Chem. Res. Toxicol. 15*, 127–139.
(47) Saparbaev, M., Langouet, S., Privezentzev, C. V., Guengerich, F. P., Cai, H., Elder, R. H., and Laval, J. (2002) 1,N^2-Ethenoguanine, a mutagenic DNA adduct, is a primary substrate of *Escherichia coli* mismatch-specific uracil-DNA glycosylase and human alkylpurine-DNA-N-glycosylase. *J. Biol. Chem. 277*, 26987–26993.
(48) Singer, B., Antoccia, A., Basu, A. K., Dosanjh, M. K., Fraenkel-Conrat, H., Gallagher, P. E., Kusmierek, J. T., Qiu, Z. H., and Rydberg, B. (1992) Both purified human 1,N^6-ethenoadenine-binding protein and purified human 3-methyladenine-DNA glycosylase act on 1,N^6-ethenoadenine and 3- methyladenine. *Proc. Natl. Acad. Sci. U.S.A. 89*, 9386–9390.
(49) Hang, B., Medina, M., Fraenkel-Conrat, H., and Singer, B. (1998) A 55-kDa protein isolated from human cells shows DNA glycosylase activity toward 3,N^4-ethenocytosine and the G/T mismatch. *Proc. Natl. Acad. Sci. U.S.A. 95*, 13561–13566.
(50) Huffman, J. L., Sundheim, O., and Tainer, J. A. (2005) DNA base damage recognition and removal: New twists and grooves. *Mutat. Res. 577*, 55–76.
(51) Wang, Y., Saleh, S., Marnett, L. J., Egli, M., and Stone, M. P. (2008) Insertion of dNTPs opposite the 1,N^2-propanodeoxyguanosine adduct by *Sulfolobus solfataricus* P2 DNA polymerase IV. *Biochemistry* [Online early access]. DOI: 10.1021/bi800152j. Published Online: Jun 19, 2008. in press.

TX8001466